

Elsevier required licence: © 2017

This manuscript version is made available under the CC-BY-NC-ND 4.0 license

<http://creativecommons.org/licenses/by-nc-nd/4.0/>

The definitive publisher version is available online at

<https://doi.org/10.1016/j.desal.2016.11.004>



21 **Abstract**

22 A better understanding of large spiral wound forward osmosis (SW FO) module  
23 operation is needed to provide practical insight for a full-scale FO desalination plant. Therefore,  
24 this study investigated two different 8” SW FO modules (i.e. cellulose tri acetate, CTA and  
25 thin film composite, TFC) in terms of hydrodynamics, operating pressure, water and solute  
26 fluxes, fouling behaviour and cleaning strategy. For both modules, a significantly lower flow  
27 rate was required in the draw channel than in the feed channel due to important pressure-drop  
28 in the draw channel and was a particularly critical operating challenge in the CTA module  
29 when permeate spacers are used. Under FO and pressure assisted osmosis (PAO, up to 2.5 bar)  
30 operations, the TFC module featured higher water flux and lower reverse salt flux than the  
31 CTA module. For both modules, fouling tests demonstrated that feed inlet pressure was more  
32 sensitive to foulant deposition than the flux, thus confirming that FO fouling deposition occurs  
33 in the feed channel rather than on the membrane surface. Osmotic backwash combined with  
34 physical cleaning used in this study confirmed to be effective and adapted to large-scale FO  
35 module operation.

36

37 **Keywords**

38 Spiral wound module; Forward osmosis; Pressure-drop; Pressure assisted osmosis; Organic  
39 fouling; Osmotic backwash

## 40 **1. Introduction**

41 The most commonly used desalination technologies are generally pressure-based  
42 membrane processes such as reverse osmosis (RO) and nanofiltration (NF). However, the  
43 wider development of these processes is often limited due to high membrane fouling and  
44 scaling propensity and high energy consumption, resulting in operation and maintenance costs  
45 [1-3]. As a potentially more sustainable alternative, the use of forward osmosis (FO) has been  
46 recently put forward and extensively investigated. In FO, the driving force is an osmotic  
47 pressure gradient, allowing water to naturally flow from a low chemical potential feed solution  
48 (FS) to a concentrated high chemical potential draw solution (DS) through a semipermeable  
49 membrane [4, 5]. Although direct cost comparison of FO with conventional NF and RO  
50 systems remains a challenging task, several studies have demonstrated that desalination by FO  
51 could lead to lower energy consumption, reduced fouling propensity and higher cleaning  
52 efficiency [5-7].

53 Recent interest in FO applications has been particularly driven by the performance  
54 improvement offered by the latest generation of FO membranes. The improvements include  
55 higher water permeability, greater selectivity and rejection, smoother active layer surface  
56 allowing lower fouling propensity, and quite importantly, a specifically adapted porous support  
57 layer offering low internal concentration polarisation (ICP) yet still appropriate mechanical  
58 support for practical operation [4, 5]. The first commercially available and specifically tailored  
59 FO membranes, based on cellulose triacetate (CTA), were developed by Hydration Technology  
60 Innovations (HTI, Albany, OR), and have been examined in various applications by numerous  
61 research groups [8-13]. More recently, thin film composite (TFC) FO membranes were  
62 designed with a polyamide selective layer, and these feature higher water flux and better solute  
63 rejection compared to CTA membranes [14-17]. In addition, TFC membranes were found to  
64 be more pH stable and were more resistant to hydrolysis and biological degradation [17-19].

65 In contrast, previous studies have reported that TFC membranes showed higher fouling  
66 tendency than CTA membranes due to the increased surface roughness [17, 18, 20, 21]. As  
67 such opportunities to increase flux with commercially available membrane exists, but long-  
68 term fouling studies are required. An optimised FO module design is expected to feature high  
69 membrane packing density, lower concentration polarization (i.e., high mass transfer  
70 coefficient) and high water permeation [22]. Performance of several commercial FO  
71 membranes (i.e., Porifera and Toyobo) has been widely reported in the literature on small  
72 membrane samples but information regarding module design is still limited since most  
73 commercial FO membrane modules are still under development. Only the performance of SW  
74 FO modules developed by HTI has been reported for a variety of feed and draw spacers (fine,  
75 medium and corrugated spacer) [12] while detailed information on other suppliers module  
76 configurations are not available. This clearly indicates that CTA and TFC membrane modules  
77 were the most mature and developed membranes during the time of this FO study. In this regard,  
78 most studies so far were conducted using small flat sheet membrane coupons which are not  
79 always representative of behaviour in full-scale modules. Therefore, a better understanding of  
80 FO behaviour in larger modules is needed to provide more practical insight for full-scale FO  
81 operation.

82

83

84 **Table 1.** Commercial development of FO membranes [12]

Company	Type	Status	FO performance		
			DS/FS	$J_w, \text{Lm}^{-2}\text{h}^{-1}\text{bar}^{-1}$	$J_s/J_w, \text{g.L}^{-1}$
HTI	CTA flat-sheet	commercial	1 M NaCl/DI	10.1	0.5
HTI	TFC flat-sheet	commercial	1 M NaCl/DI	10	0.8
Oasys	TFC flat-sheet	pre-commercial	1 M NaCl/DI	30	0.7
Aquaporin	AqP flat-sheet	pre-commercial	1 M NaCl/DI	9.5	-
Porifera	PFO flat-sheet elements	commercial	1 M NaCl/DI	33.0	0.2-0.6
Samsung	Hollow fibre	development	1 M KCl/DI	9.3	0.6
Toyobo	Hollow fibre	commercial	-	-	-

85

86 A large-scale spiral wound (SW) FO module typically requires four ports: two inlets  
87 and two outlets for both the FS and DS. In SW FO modules, the FS circulates in the feed  
88 channel between the rolled layers, and the DS flows through the central tube into the inner side  
89 of the membrane envelop [23]. Therefore, flow patterns and flow resistance in the feed and  
90 draw channels can be different and affected by specific module design. In particular, a more  
91 detailed study linking operating conditions (flow rates, inlet pressures) to resulting  
92 performances (water flux, reverse salt flux, fouling and cleaning efficiency) of SW FO modules  
93 will provide important insights in the operability of current SW FO modules on full-scale.

94 Very limited pilot-scale FO studies using SW FO modules currently exist in literature  
95 [23-25]. However, these pilot studies are of crucial importance for further FO development  
96 since the operation of SW modules in industrial plants is affected by several factors such as the  
97 number of membrane leaves, feed and draw channel height, spacers that affect mass transfer  
98 and pressure loss, but also fouling potential [26]. To the best of the author's knowledge, so far  
99 only two studies have been reported in literature using 4040 SW (4" in diameter and 40" in  
100 length) [24] and 8040 SW (8040, 8" inch in diameter and 40" in length) [23] HTI CTA FO

101 modules. Those studies mainly focused on the optimisation of a large-scale SW FO module  
102 [24] and of a newly proposed fertiliser drawn forward osmosis process for a specific application  
103 [23, 27]. However, the susceptibility of SW FO modules to membrane fouling during the long-  
104 term FO operation has not been considered in those studies, which could consequently  
105 exacerbate the performance of in full-scale FO stand-alone or hybrid process. Although  
106 membrane fouling on the feed side in FO happens less and is easily removed by simple physical  
107 cleaning [3, 28, 29], the effect of osmotic backwash seems to be unclear. Some studies have  
108 reported that the osmotic backwash could lead to an adverse effect on the driving force due to  
109 the accumulation of the reversed solutes within the fouling layer [29-31]. Nevertheless, the  
110 specific combination of osmotic backwash with subsequent physical cleaning could be more  
111 effective to restore a significant portion of water productivity after fouling occurred [32]. Thus,  
112 there is a critical need to control operating conditions and assess performances of SW FO  
113 modules more systematically including fouling behaviour and cleaning strategies for  
114 sustainable FO operation.

115 As an alternative to FO, a new FO-derived concept called pressure assisted osmosis  
116 (PAO) has recently been developed. PAO is aimed at increased water production compared to  
117 FO for more favourable economics for further commercialization [32-36]. In PAO, hydraulic  
118 pressure is applied on the feed side of the membrane to enhance the water flux through the  
119 synergistic effects of hydraulic pressure and osmotic pressure [32-36]. Overall, it has been  
120 demonstrated that by increasing the applied pressure, the water flux was significantly improved  
121 despite higher ICP. Even more than for FO, the role of a spacer in the PAO process is important  
122 to prevent the deformation and damage of the membrane caused by the applied hydraulic  
123 pressure on the feed side of the membrane [34, 36, 37]. This reinforces the need to evaluate the  
124 impact of hydraulic pressure on the module-scale FO and PAO operations.

125           Accordingly, there is a clear need for a detailed assessment of the impact of  
126 hydrodynamic conditions on pressure behaviour of an SW FO module (i.e. build-up in draw  
127 stream and drop along feed line). This study therefore systematically studied the performances  
128 of two commercial SW FO modules (CTA from HTI and TFC from Toray Industries Inc). An  
129 assessment of the water flux and reverse salt flux behaviours as a function of operating  
130 conditions in both FO and PAO operation was conducted to evaluate the performance of both  
131 modules compared to lab-scale experiments. Fouling studies were performed with a mixture of  
132 model organic foulants was then used to evaluate the fouling behaviour and cleaning strategies  
133 for the modules operated in a seawater dilution application. To our best knowledge, this is the  
134 first study addressing the practical operations of commercially available 8” SW FO modules  
135 and providing a comparative assessment of long-term fouling behaviour in large-scale FO  
136 process. Therefore, the results reported in this study can be useful for further investigation of  
137 the fouling control by chemical cleaning and/or pre-treatment in full-scale FO operation.

138

## 139 **2. Material and Methods**

### 140 **2.1. Spiral wound FO membrane module**

141           Two different 8” SW FO modules were used (Table 2): one CTA module manufactured  
142 by HTI and one TFC polyamide module manufactured by Toray Industries, Korea. In both  
143 modules, the rejection layer of the membrane faces the FS and the porous support layer of the  
144 membrane faces to the DS. Feed and permeate spacers were present to keep the membrane  
145 leaves apart [23, 24].

146           As presented in Table 2, the CTA module had a corrugated feed spacer made of 2.5 mm  
147 polystyrene chevron and an effective membrane area of 9 m<sup>2</sup> with six membrane leaves. The  
148 TFC module had a feed spacer made of a 1.19 mm diamond type polypropylene mesh and an  
149 effective membrane area of 15 m<sup>2</sup> with ten membrane leaves. In addition, both modules had


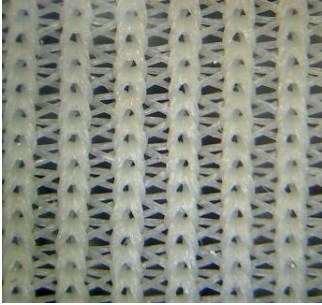
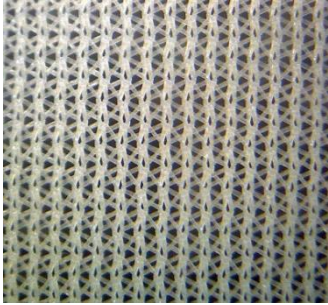


150 different permeate spacers: the CTA module had three tricot spacers, while the TFC module  
151 featured a draw channel containing one diamond type spacer wedged in between two tricot  
152 type spacers. If a net spacer is used inside of the envelope in the SW FO module and the DS  
153 side is pressurized, the feed flow channel may be blocked by membrane deformation.  
154 Accordingly, a tricot fabric spacer is used inside the envelope like a permeate carrier of an SW  
155 RO module and prevents the membrane deformation and this structure has been already utilised  
156 for pressure-retarded osmosis application [38]. Water permeability (A) for both FO modules  
157 was measured in RO mode in a pilot-scale FO unit (tap water - conductivity  $240 \pm 20 \mu\text{m}/\text{cm}$   
158 - in the feed and draw sides). The tests were conducted at increasing feed pressures (in intervals  
159 of 0.5 bar up to 2.5 bar).  $A_{\text{CTA}}$  and  $A_{\text{TFC}}$  were found to be  $1.6 \pm 0.2$  and  $8.9 \pm 0.14 \text{ Lm}^{-2}\text{h}^{-1}\text{bar}^{-1}$   
160 <sup>1</sup>, respectively. Additional information on the properties of the CTA and TFC FO membranes  
161 such as water and salt permeability (A and B values), feed rejection (R), structural parameter  
162 (S) and membrane total thickness are all provided in the Table S2 in the Supplementary  
163 Information.

164

165

166 **Table 2.** Specifications of two spiral wound forward osmosis membrane modules employed in  
 167 this study.

Parameter	CTA (HTI)	TFC (Toray)
Effective membrane area, m <sup>2</sup>	9	15
Number of leaves in the assembly	6	10
Feed spacer thickness, mm	2.5	1.19
Feed spacer type	Corrugated polystyrene	Diamond polypropylene
*Image of feed spacer	n.a.	
Draw spacer type	Tricot(dense/rigid)	Tricot(flexible)/Diamond
*Image of draw spacer		
Water permeability(A), Lm <sup>-2</sup> h <sup>-1</sup> bar <sup>-1</sup>	1.6 ± 0.2	8.9 ± 0.1

168 \*Microscope measurement (5MP USB 2.0 Digital Microscope) and the spacers obtained from  
 169 the SW FO module autopsy.

170

## 171 2.2. Feed and draw solutions

172 A draw solution at a concentration of 35 g/L of Red Sea salt (RSS) from Red Sea Inc.  
 173 with an equivalent osmotic pressure of 24.7 bar was prepared and used in all experiments [32,  
 174 33]. RSS composition is described in Table S1 in the Supplementary Information. Humic acid  
 175 and alginate were chosen as model organic foulants, while calcium (as calcium chloride, CaCl<sub>2</sub>)  
 176 was added to further enhance fouling. Model organic foulants used in this study have been  
 177 known as major organic components in wastewater and have extensively been used to study in  
 178 fouling behaviour in FO process [32, 39, 40]. In fouling experiments, the FS was prepared by  
 179 mixing the following chemicals to tap water: 1.2 g/L RSS, 0.22 g/L CaCl<sub>2</sub> (Ajax Finechem Pty

180 Ltd, Tarend point, Australia), 0.2 g/L humic acid sodium salt (Aldrich, Milwaukee, WIS) and  
181 0.2 g/L alginic acid sodium salt (Sigma Aldrich Co., St Louis, MO). The total organic carbon  
182 (TOC) concentration of the feed was 94 mg/L. Before and after the fouling experiments,  
183 baseline experiments were conducted using tap water and 35g/L RSS as FS and DS,  
184 respectively.

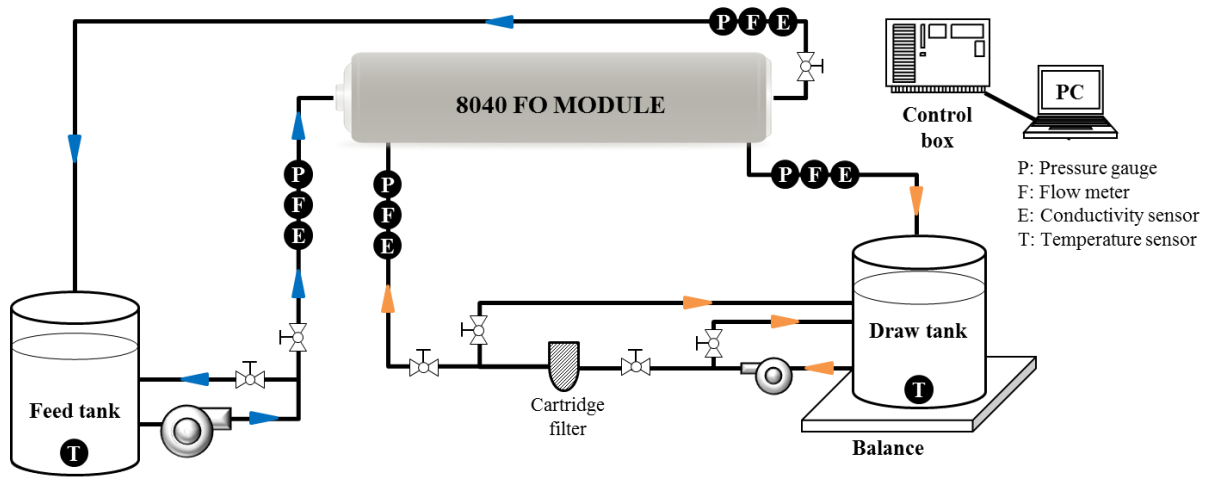
185

### 186 **2.3. Pilot-scale system and experimental procedure**

187 As shown in Fig. 1, a pilot-scale FO system was used for the experiments. Details about  
188 the design and control of the pilot-scale FO system are provided in our previous study [23].  
189 Flow meters, pressure gauges and electrical conductivity (EC) meters were installed at both the  
190 inlet and outlet points of the module and connected to a computer for online data recording and  
191 monitoring. Although the feed and draw flow rates were varied between 17 and 100 L/min and  
192 between 4 and 15 L/min, respectively, the cross-flow velocity of each module shows difference  
193 due to their different module designs. The converted feed and draw cross-flow velocities for  
194 both are presented in Table 3.

195 The impact of feed and draw flow rates on pressure-drop were successively evaluated.  
196 For this evaluation, 500 L of FS and DS were prepared with tap water, and each experiment  
197 was carried out at a fixed draw flow rate, while the feed flow rate was varied and vice versa.  
198 Details of the experiment conditions are summarized in Table 3.

199



**Fig. 1.** Schematic diagram of the pilot-scale FO experimental set up and illustration of 8040 spiral wound FO modules: (a) CS CTA and (b) MS TFC (CS: corrugated feed spacer and MS: medium diamond shape feed spacer).

200

201 **Table 3.** Experimental conditions for module hydrodynamic tests.

Module	Test No.	Feed cross-flow velocity, m/s (L/min)	Draw cross-flow velocity, m/s (L/min)	FS and DS
CTA	Test 1	0.08-0.44 (17-100)	0.04 (10)	Tap water of 500 L
	Test 2	0.18 (40)	0.02-0.07 (4-15)	
TFC	Test 3	0.16-0.91 (17-100)	0.09 (10)	
	Test 4	0.37 (40)	0.04-0.14 (4-15)	

202

203 PAO operation was also tested to assess the effect of the hydraulic pressure in the feed  
 204 channel. Feed pressure was changed by adjusting the back pressure valve for fixed feed and  
 205 draw flow rates. The maximum operating pressure used in this study was 2.5 bar as feed inlet  
 206 pressure. The PAO experiments were performed with 200 L of 35 g/L RSS as DS and 500 L  
 207 of tap water as FS. The feed and draw flow rates were constant and fixed based on the optimised  
 208 conditions defined in the initial SW FO module experiments.

209

210 Water fluxes ( $J_w, \text{Lm}^{-2}\text{h}^{-1}$ ) were calculated by using the following formula:

211

212 
$$J_w = \frac{\text{Change in DS volume (L)}}{A_m(\text{m}^2) \times \Delta t (\text{hr})}$$

213

214 where  $A_m$  is the effective membrane surface area ( $\text{m}^2$ ) and  $\Delta t$  is the operation time (hr). In  
 215 addition, the recovery rate (%) during the operation in FO and PAO modes was defined as

216

217 
$$\text{Recovery rate} = \frac{\text{Permeated volume (PV, L)}}{\text{Initial FS volume (L)}} \times 100$$

218

219 When tap water was used as FS in FO and PAO modes, the change in FS salt concentration  
 220 (and thus reverse salt flux) was determined based on conductivity measurements (using a  
 221 multimeter CP-500L, ISTEK, Korea) [6]. The concentration change in the feed solution at the  
 222 beginning and end of each experiment was measured. The measured value was used to calculate  
 223 the specific reverse solute flux (SRSF), which is defined as a ratio of reverse salt flux ( $J_s$ ,  $\text{gm}^{-2}\text{h}^{-1}$ )  
 224 and water flux ( $J_w$ ,  $\text{Lm}^{-2}\text{h}^{-1}$ ) [34, 41]. SRSF ( $J_s/J_w$ ,  $\text{g/L}$ ) was then calculated using the  
 225 following formula:

226

227 
$$\text{SRSF} = \frac{1}{J_w} \left( \frac{C_f V_f - C_i V_i}{A_m \Delta t} \right)$$

228

229 where  $C_i$  and  $C_f$  are the initial and final feed solute concentration ( $\text{g/L}$ ), and  $V_i$  and  $V_f$  are the  
 230 initial and final volume of the feed water (L). When DI water was used as FS, the RSF/SRSF  
 231 was determined by measuring the increased electrical conductivity of the FS between the start  
 232 and end of each batch experiment. The electrical conductivity was then converted into mass  
 233 concentration using calibration curve for the RSS concentration versus conductivity as shown  
 234 in Fig. S1 in the Supplementary Information.

235

## 236 **2.4. Fouling cycles and cleaning experimental procedure**

237 Fouling behaviour was evaluated in FO operation (no hydraulic pressure added, i.e.  
238 back pressure valve opened) for both modules. All experiments were conducted with 200 L of  
239 35 g/L RSS as DS and 500 L mixed fouling solution (as described in Section 2.2) as FS. After  
240 400 L of water permeated (i.e. after 80% recovery feed water reached), the test was stopped  
241 and new feed and draw solutions were prepared and a new fouling cycle was initiated (without  
242 cleaning in-between cycles). Fouling runs were repeated for three cycles in total, before  
243 cleaning took place. Operation time for the CTA module was much longer than for the TFC  
244 module due to its low water permeability (since similar permeation volumes were aimed at).

245 Osmotic backwashing was conducted after the three fouling cycles, using 200 L of 35  
246 g/L RSS as cleaning DS (replacing the feed water) and tap water as cleaning feed solution  
247 (replacing the DS) for 60 min to remove the fouling layer from the membrane surface at the  
248 same feed and draw flow rates of 40 and 10 L/min, respectively for both modules (cross-flow  
249 velocities for each module are shown in Table 2). After the osmotic backwash, physical  
250 cleaning at 100 L/min of feed flow rate (0.44 and 0.91 m/s for CTA and TFC modules,  
251 respectively) was performed for 5 min using tap water to flush the dislodged foulants from the  
252 feed channel [32]. During the physical cleaning, samples of the feed side (used as draw side  
253 during the backwashing) were collected every 1 min (100 L flushing), and analysed using a  
254 total organic carbon (TOC) analyser (SGE Anatoc TOC II Analyser). Before each fouling run,  
255 as well as before and after cleaning, the baseline flux was measured by operation with tap water  
256 as FS and 35 g/L as DS for 30 min to assess the influence of fouling on membrane permeability  
257 and inlet pressure (and pressure-drop) in the feed channel.

258

## 259 **3. Results and discussion**

## 260 **3.1. Impact of operating conditions on module hydrodynamics**

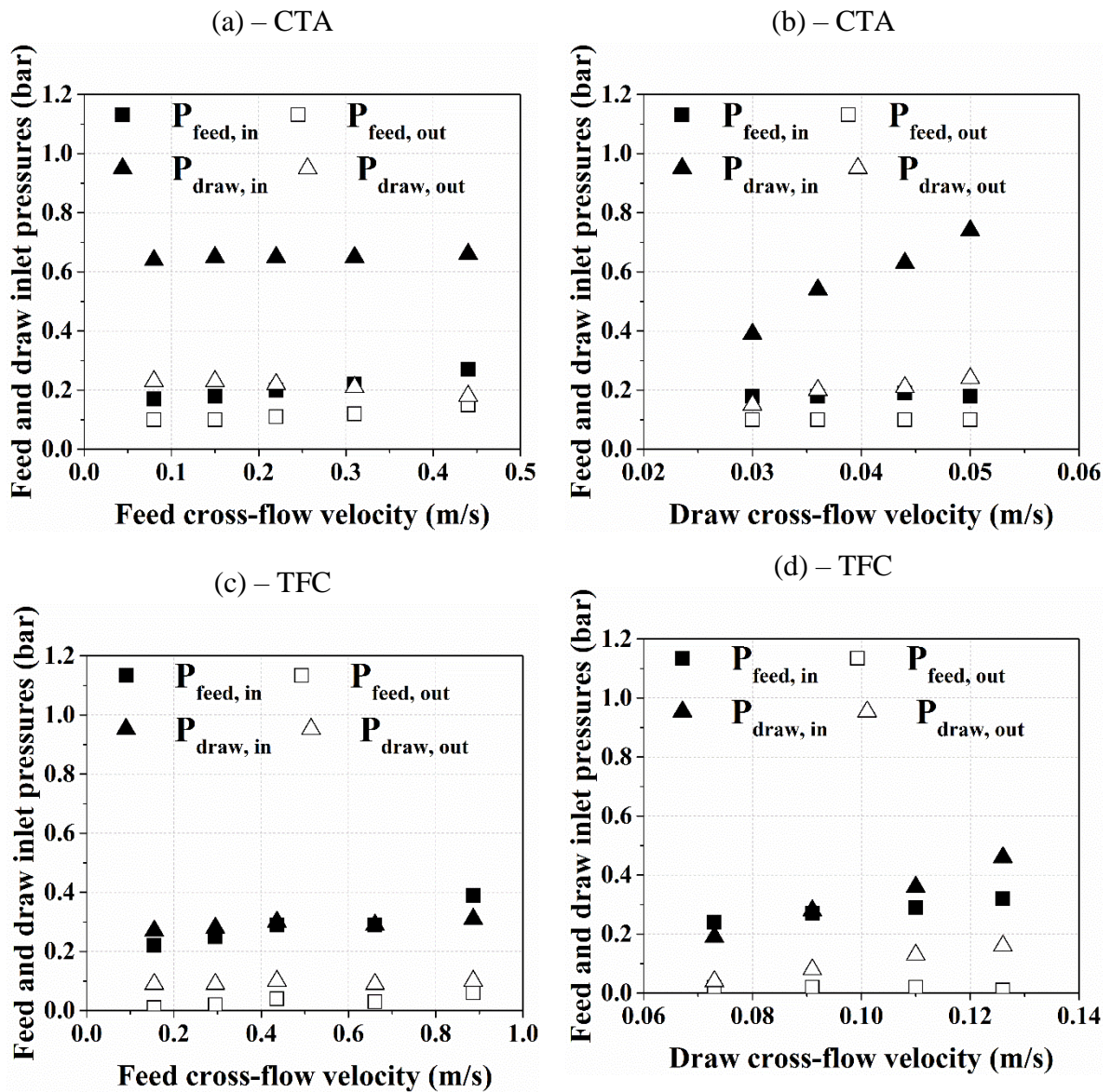
### 261 **3.1.1. Impact of feed and draw flow rates on pressure-drop (without permeation)**

262 It should be noted that the flow rate range is much lower in the draw channel, as  
263 recommended in [23, 24]. Results for the CTA module (Fig. 2 (a)) indicate that the effect of  
264 feed flow rate increase on the pressure-drop was moderate (at constant draw cross-flow velocity  
265 of 0.04 m/s). When the feed cross-flow velocity was increased from 0.08 to 0.44 m/s, the feed  
266 inlet pressure was increased from 0.17 to 0.27 bar. In addition, as shown in Fig. 2 (b), when  
267 the draw cross-flow velocity was increased from 0.03 to 0.05 m/s (much lower range than for  
268 feed stream), the draw inlet pressure was more linearly increased from 0.39 to 0.74 bar. This  
269 demonstrates that much higher flow resistance occurs in the draw channel of the CTA module,  
270 which is mainly due to the use of dense and thick draw tricot spacers with lower cross-flow  
271 velocities in both sides of the module (Tables 1 and 2) [42].

272 When the feed cross-flow velocity was increased from 0.16 to 0.91 m/s in the TFC  
273 module (Fig. 2 (c)), the feed inlet pressure was increased from 0.22 to 0.39 bar. Specifically,  
274 under much higher feed cross-flow velocity of 0.91 m/s (Table 2), the feed inlet pressure with  
275 the TFC module is slightly higher (0.39 bar) than that with the CTA module (0.27 bar), which  
276 corroborates with the fact that the spacer used in the feed channel of the TFC module is thinner  
277 (1.19 mm) with higher packing density leading to lower feed channel height (0.00258 mm for  
278 TFC and 0.00394 mm for CTA), resulting in higher feed inlet pressure [26, 43, 44]. Pressure-  
279 drop in the draw channel of the TFC module was not only lower but also much less sensitive  
280 to flow rate variation than in the CTA module, mainly due to the presence of one layer of  
281 diamond spacer with much lower resistance in the draw channel (Fig. 2 (d)).

282 As such, it is clear that spacer design is of crucial importance for pressure-drop in the  
283 SW FO module. The tested CTA module with a corrugated spacer in the feed channel does  
284 allow a very low pressure drop in the feed channel, but this comes at the cost of a low packing

285 density. Most likely, this is only justifiable economically if feed waters with a very high load  
 286 of foulants and potential clogging problems is treated. In that aspect, the diamond spacer used  
 287 in the TFC module appears to be a better compromise that allows for higher packing densities  
 288 at moderate pressure drop. The permeate spacers used in the CTA module resulted in a very  
 289 large pressure drop, even at low flow rate. Combinations of tricot permeate spacers to support  
 290 the membrane and limit deformation and a diamond spacer to limit pressure-drop (as in the  
 291 TFC module) (Table 1) allows using higher draw flow rates.  
 292





**Fig. 2.** Effect of feed and draw cross-flow velocities on pressure build-up in CTA (a and b) and TFC (c and d) modules. Tap water was used as FS and DS.

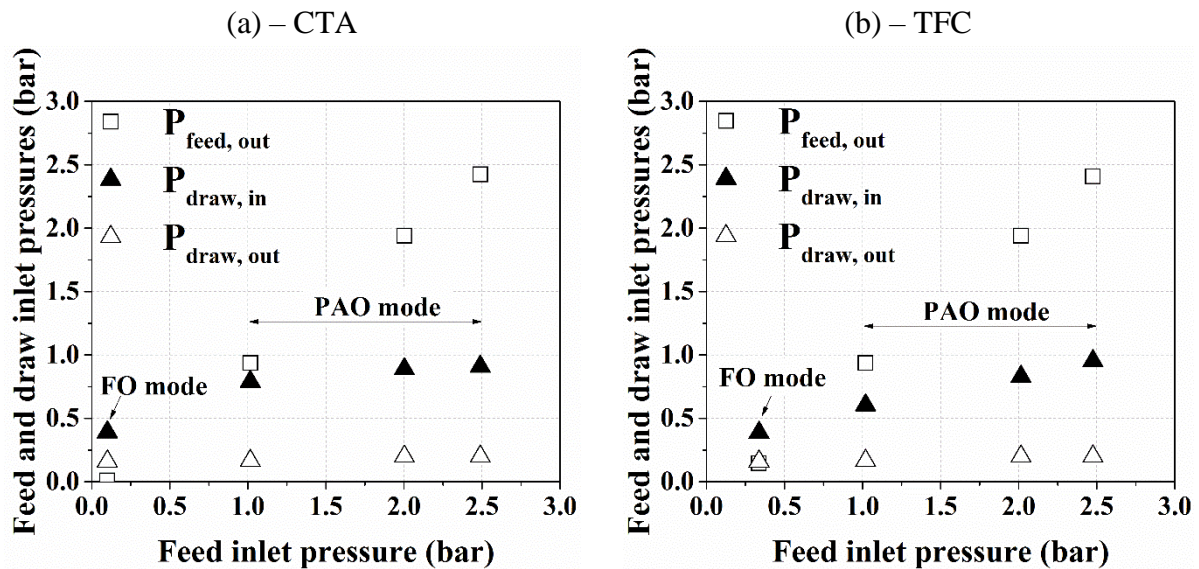
293

### 294 **3.1.2. Impact of feed and draw channel pressurisation on pressure-drop**

295 In these experiments, the system was operated by adjusting the feed inlet pressure using  
296 the back pressure valve of the feed side. Fig. 3 shows the impact of the feed inlet pressure on  
297 the feed and draw channel inlet and outlet pressures for both modules. For both modules (Figs.  
298 3 (a) and (b)), the draw inlet pressure was increased when pressure was applied on the feed  
299 side. Interestingly, both modules have very distinct behaviour with regards to this “pressure  
300 transfer.” For the CTA module, the draw inlet pressure increase is already maximal at lower  
301 hydraulic pressures (1 bar), and remains constant even when further increasing the feed  
302 pressure (up to 2.5 bar). This appears to indicate that the pressurisation of the draw side in the  
303 CTA module is more likely a consequence of draw channel pressurisation on the tricot type  
304 support on the draw side. At higher pressures, further reduction of the channel is not possible  
305 as the tricot support could not be more compacted. For the TFC module, a more linear increase  
306 in the draw inlet pressure was observed with increasing feed pressure (Fig. 3 (b)). Here, it could  
307 thus be hypothesized that the diamond type spacer is less supportive and allows for more  
308 channel reduction [33, 45]. To identify the reason behind the increases in draw pressure for  
309 both modules, RO tests with the modules were compared to tests in FO mode (using tap water  
310 as FS and DS).

311

312



**Fig. 3.** Impact of feed inlet pressure on the feed and draw channel pressurisation with (a) CTA and (b) TFC modules. Feed cross-flow velocity was constant at 0.18 m/s for CTA and 0.37 m/s for TFC, while the draw flow cross-flow velocities for CTA and TFC modules were 0.04 and 0.09 m/s, respectively. Tap water was used as FS and DS.

314

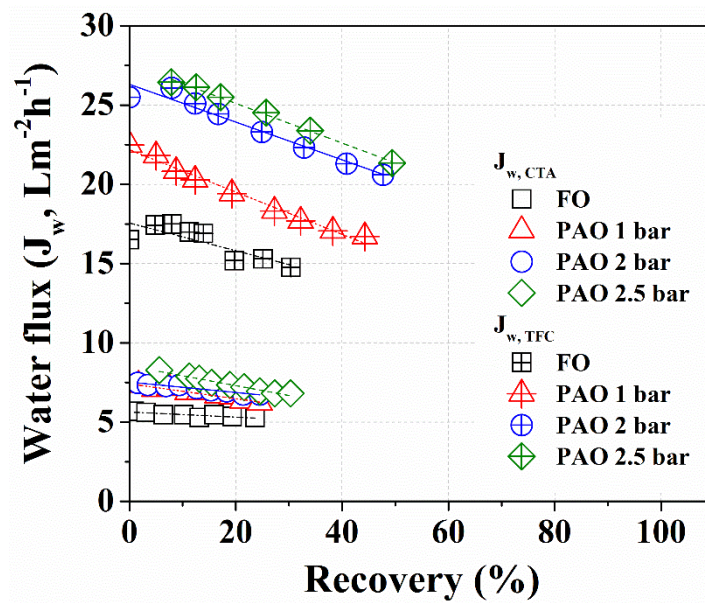
### 315 **3.2. Relative contribution of hydraulic pressure to permeation flux**

316 FO and PAO tests were carried out using CTA and TFC modules (Fig. 4), and now with  
 317 tap water as FS, and 35 g/L RSS as DS. The water fluxes in FO and PAO modes with the TFC  
 318 module were significantly higher than that with the CTA module. For example, in FO mode  
 319 (no hydraulic pressure applied), the flux with the TFC module was around  $16.6 \text{ Lm}^{-2}\text{h}^{-1}$ , while  
 320 the flux with the CTA module was around  $5.4 \text{ Lm}^{-2}\text{h}^{-1}$ . The higher performance of the TFC  
 321 membranes compared to CTA membranes corroborates findings from literature [16, 46].

322 In PAO mode (Fig. 4), as expected, the water flux improved with increasing applied  
 323 pressures. For the CTA module, the flux increase with applied pressure was moderate, i.e.,  
 324 from  $6.72$  to  $7.3 \text{ Lm}^{-2}\text{h}^{-1}$  (at 2.5 bars of applied pressure) and remained much lower than the  
 325 fluxes obtained with the TFC module. For the TFC module, the impact of the applied pressure  
 326 on the water flux was significant, already at low applied pressure (flux increased from 19 to  
 327  $24.5 \text{ Lm}^{-2}\text{h}^{-1}$  at 1 and 2.5 bar, respectively). This confirms that the TFC membranes not only

328 has higher permeation flux in FO mode, but is also more responsive to the use of hydraulic  
 329 pressure (PAO mode) due to its higher water permeability. Although additional energy is  
 330 required to pressurise the feed solution in PAO, the significant increase in performance could  
 331 lead to additional cost savings, in particular by a reduction of the number of membrane modules  
 332 required [47].

333



**Fig. 4.** Comparison of flux behaviour in pilot-scale FO and PAO processes using two different SW FO modules. Experimental conditions: feed flow rate: 0.18 and 0.37 m/s for CTA and TFC, respectively, draw flow rate: 0.04 m/s for CTA and 0.09 m/s for TFC, and applied pressure in PAO: 1, 2 and 2.5 bar, 35 g/L RSS as DS and tap water as FS.

334

335 Table 4 shows the comparison of the specific reverse salt flux (SRSF) behaviour for  
 336 FO and PAO modes using the two different SW FO modules. Compared to the CTA module,  
 337 the TFC module had much lower SRSF, and thus not only had a higher flux but also a higher  
 338 selectivity than the CTA module. As expected from the previous lab experiments, the results  
 339 show a significant decrease in the SRSF for both modules with increasing applied pressure.  
 340 For example, the SRSF were 1.22 and 0.37 g/L for CTA and TFC, respectively in FO mode,  
 341 and decreased down to 0.64 and 0.10 g/L for CTA and TFC, respectively in PAO mode with a  
 342 feed inlet pressure of 2.5 bar [33, 34, 36]. This corroborates previous findings that reverse

343 transport of the draw solutes through the membranes is significantly decreased by the enhanced  
344 water permeation. The effect of hydraulic pressure on the RSF for the TFC is even more  
345 propounded compared to the CTA, due to the higher water permeability of the TFC. Also, the  
346 CTA module could have the risk of irreversible fouling on the support layer caused by more  
347 solute diffusing from DS into FS in which the enhanced salt accumulation on the feed side of  
348 the CTA module and is mainly promoted by the reverse diffusion of Na<sup>+</sup> [48, 49]. Such reverse  
349 solute flux through the FO membranes can have significant economic impact on the FO  
350 process. Draw solute leakages through SRSF in the FO process is one of the major contributors  
351 to draw solute replenishment cost in a continuous closed-loop configuration [50]. A recent  
352 study conducted by Phuntsho et al [51] has pointed out that accumulation of draw solutes in  
353 the feed brine would be one of the significant environmental challenges for brine disposal,  
354 especially for FO membranes with lower reverse flux selectivity. This indicates that, CTA with  
355 lower reverse flux selectivity (as shown in Table 4) would result in much higher accumulation  
356 of draw solutes in the feed brine thus leading to higher draw replenishment and brine treatment  
357 costs. These studies clearly show that the TFC FO membrane with much higher reverse flux  
358 selectivity than CTA FO membrane would be more beneficial for FO hybrid systems.

359

360 **Table 4.** Comparison of specific reverse salt flux (SRSF,  $J_s/J_w$ ) behaviour in pilot-scale FO  
361 and PAO processes using two different SW FO modules: CTA and TFC.

Operation mode	CTA module			TFC module		
	$J_w, \text{CTA}$ ( $\text{Lm}^{-2}\text{h}^{-1}$ )	$J_s, \text{CTA}$ ( $\text{gm}^{-2}\text{h}^{-1}$ )	$J_s/J_w$ ( $\text{g/L}$ )	$J_w, \text{TFC}$ ( $\text{Lm}^{-2}\text{h}^{-1}$ )	$J_s, \text{TFC}$ ( $\text{gm}^{-2}\text{h}^{-1}$ )	$J_s/J_w$ ( $\text{g/L}$ )
FO	5.4	6.58	1.22	16.6	6.1	0.37
1 bar	6.7	6.12	0.91	19.0	4.1	0.22
PAO 2 bar	7.1	5.47	0.77	23.6	2.6	0.11
2.5 bar	7.3	4.66	0.64	24.5	2.5	0.10

362

363

364

### 365 **3.3. Fouling behaviour in SW FO modules and impact on hydraulic performance**

366 The water flux as a function of permeate volume is presented in Fig. 5 (a) and (c) while  
367 permeate volume and recovery rate as a function of operation time is shown in Fig. 5 (b) and  
368 (d). During each batch, flux decreased significantly with time (and increasing recovery) due to  
369 a combination of the osmotic dilution of the DS and potentially fouling. Only when comparing  
370 initial permeation fluxes for batches, occurrence of fouling can be individually assessed. No  
371 significant initial permeation flux decline with batches was observed for neither of the tested  
372 modules, even after three batches of operation without cleaning in between. As such, despite  
373 the relative long time of operation, especially for the CTA module, and the high load of foulant  
374 used, a faster flux decline was noticed at early stages of operation but between fouling  
375 experiments the flux decline was relatively small (Fig 5 (a)). For the TFC module (Fig. 5 (b)),  
376 fouling was limited, although a higher impact of fouling was initially expected due to the higher  
377 roughness of the membrane and the higher permeation flow compared to the CTA [1, 52].  
378 Such little flux decline for TFC module shows that the fouling happening in the SW FO module  
379 is clearly different from the results reported in existing literature, which was conducted using  
380 small FO membrane coupons [21, 53, 54]. This study seems to suggest that the membrane  
381 surface properties play a less dominant role in SW FO module fouling.

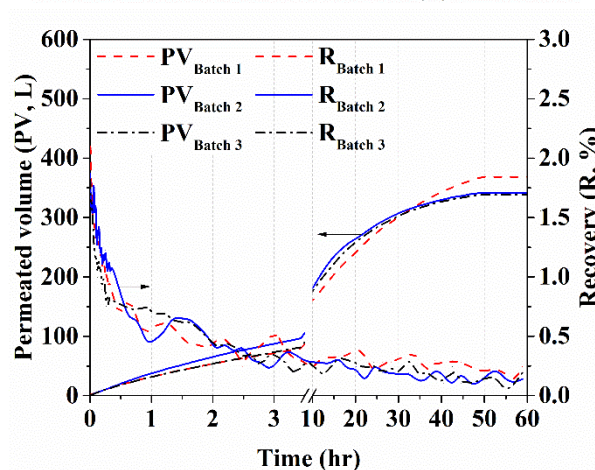
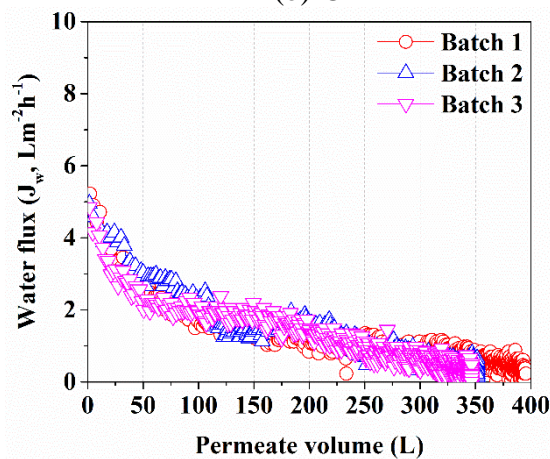
382 Nevertheless, there was the steep decrease of the initial water flux was observed with  
383 CTA module, and the initial recovery rate between the CTA and TFC modules was  
384 significantly different (recovery rate of 10 % and 2% for CTA and TFC modules, respectively),  
385 resulting in the huge difference of operation time for CTA and TFC modules (i.e. 20 times  
386 higher). This was more likely because of two reasons; the impact of ECP on the membrane  
387 surface of the CTA module mainly due to higher RSF (discussed in Section 3.2) and that the  
388 CTA module used in this study has been operating several times before we conducted the  
389 fouling experiments, thus it could already have a fouling layer on the membrane surface to

390 some extent even though the flux was almost fully restored after hydraulic cleaning [51]. More  
 391 specifically, it was observed that the recovery rate of the CTA module after 10hrs operation  
 392 was around 1% with water flux of lower than  $1 \text{ Lm}^{-2}\text{h}^{-1}$  and thus there was no meaning to  
 393 operate CTA module longer than 10 hrs (Fig. 5 (a)). From this aspect, CTA and TFC module  
 394 configuration in a full-scale FO desalination plant cannot be the same and it is dependent on  
 395 the performance of FO membrane modules. Thus, it is more preferred that CTA modules  
 396 should be paralleled in a full-scale FO desalination plant.

397

(a)-CTA

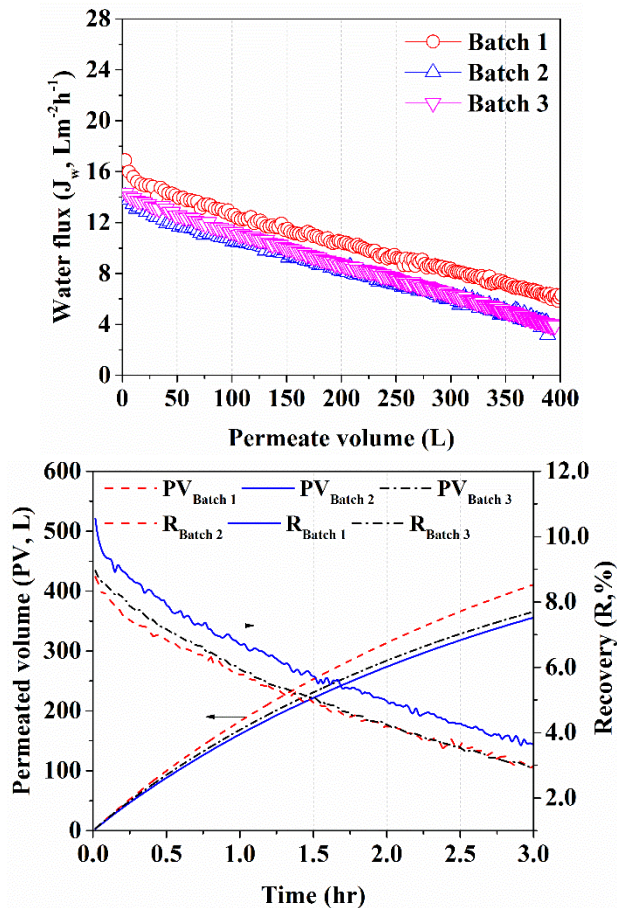
(b)-CTA



(c)-TFC

(d)-TFC





**Fig. 5.** Effect of organic foulant in feed solution on FO fouling of CTA (a and b) and TFC (c and d) modules. (a) and (c) water flux ( $J_w$ ) as a function of permeate volume (L); (b) and (d) permeate volume (L) and recovery rate (R) as a function of operation time. Fouling experiments were conducted using 35 g/L RSS as DS and feed fouling solution prepared by addition of 1.2 g/L RSS, 0.22 g/L  $CaCl_2$ , 0.2 g/L alginate, 0.2 g/L humic acid.

398

399

400

401

402

403

404

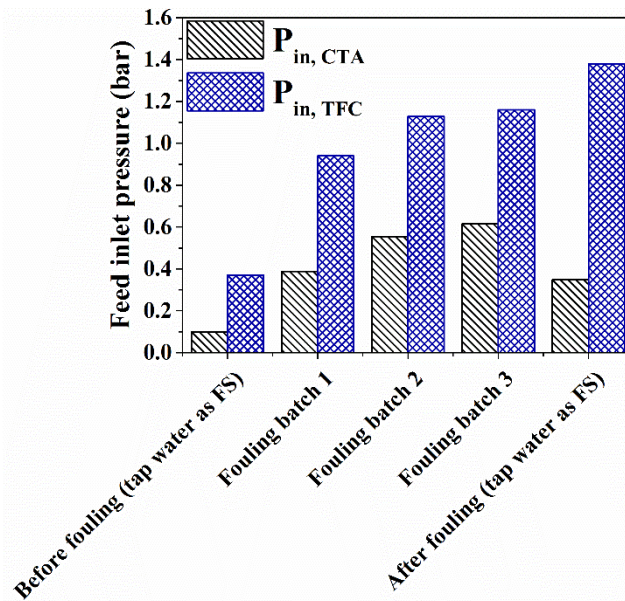
405

406

To get further insight in the behaviour of the SW FO modules during the fouling (as no real decrease in water permeability was noticed over the batches), feed inlet pressure was compared before and after the fouling experiments. Fig. 6 compares the feed inlet pressure during fouling experiments with the feed pressure using pure water as feed before and after the third batch of fouling. As shown in Fig. 6, as soon as the foulant mixture was used as FS, a much higher feed inlet pressure was observed in the module, due to higher viscosity resulting in an increase flow resistance and pressure-drop along the membrane channel on the feed side. This feed pressure increase most likely indicates foulant deposition, although no decrease in

407 permeation flux was noticed. This would indicate that fouling occurs more in the channel  
408 spacers rather than on the membrane surface. Most likely, the foulants accumulated in dead  
409 zone of the feed spacer, and consequently, the cross-flow velocity and the required pressure  
410 increased in the feed channel. Despite the fact that no decrease in membrane water permeability  
411 is seen, the increased pressure-drop in the feed channel is of course unwanted. Increased  
412 pressure drops lead to higher energy consumption for the pump to maintain the water  
413 circulation [26]. As such, controlling fouling in the feed channel, and avoiding unwanted  
414 pressure-drop will be a key parameter for real-life FO operation, especially on challenging feed  
415 streams. By comparing feed pressure (with tap water as FS) before and after fouling  
416 experiments, it is clear that for the TFC module, pressure-drop increased much more than for  
417 the CTA one (i.e. 1 and 0.25 bar, respectively). As discussed earlier, the corrugated spacer  
418 used in the CTA module leads to an increased channel thickness with lower initial pressure-  
419 drop and most likely less sensitivity to fouling deposition with much longer operation time. In  
420 addition, since the CTA module has shown lower cross-flow velocity of around 0.18 m/s  
421 compared to the TFC module (0.37 m/s) corresponding to the flow rate of 40 L/min, thus  
422 showing that mass transfer coefficient of TFC module ( $3.04 \times 10^{-5}$  m/s) is higher than that of  
423 CTA module ( $2.40 \times 10^{-5}$  m/s). Consequently, the loose fouling layer in the corrugated spacer  
424 can be flushed to some extent or changed by hydrodynamics due to its spacer geometry (Fig.  
425 6).  
426





**Fig. 6.** Feed inlet pressure change with CTA and TFC modules. Fouling experiments were conducted using 35 g/L RSS as DS and feed fouling solution prepared by addition of 1.2 g/L RSS, 0.22 g/L  $\text{CaCl}_2$ , 0.2 g/L alginate, 0.2 g/L humic acid.

427

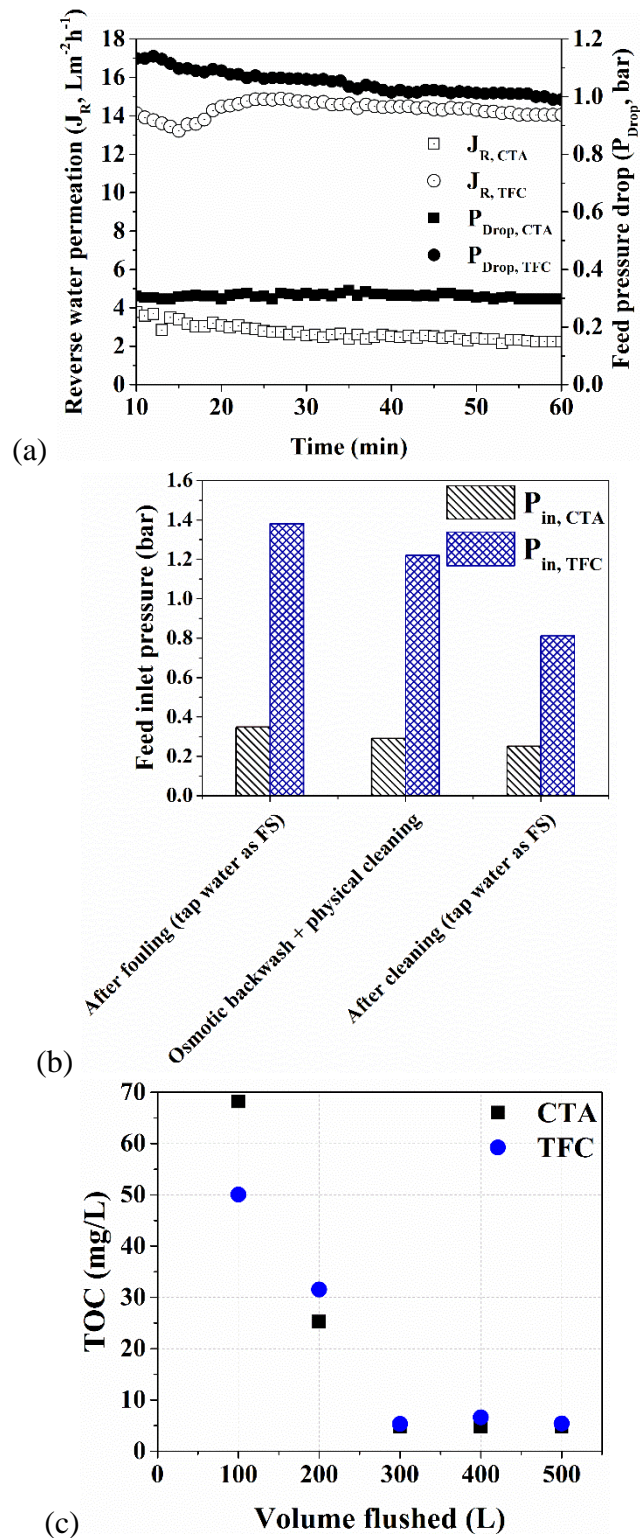
### 428 3.4. Fouling reversibility by osmotic backwash

429 As discussed in Section 3.3, no significant impact of fouling was observed on  
 430 permeation flux, indicating that fouling occurs more in the spacers rather than on the membrane  
 431 surface in the SW FO modules. Therefore, it is unclear whether osmotic backwashing will have  
 432 a clear effect on fouling remediation. To assess this, not only the water permeability was  
 433 monitored, but also the potential recovery of the pressure-drop in the feed channel. The  
 434 cleaning strategy consisted in a combination of osmotic backwash followed by feed channel  
 435 water flushing at high cross flow velocity (Section 2.4). During the osmotic backwash, the feed  
 436 pressure drop remained relatively constant for the CTA module, but was observed to decrease  
 437 slightly for the TFC module (see Fig. 7 (a)). This indicates that the osmotic backwashing could  
 438 be efficient to recover materials accumulated in the feed channel during operation, especially  
 439 for TFC membrane module. Besides, as shown in Fig. 7 (a), significant reverse flux difference  
 440 between CTA and TFC modules was observed during the osmotic backwash. For instance, the  
 441 reverse water permeation in the TFC module (average of  $14.5 \text{ Lm}^{-2}\text{h}^{-1}$ ) was much higher than

442 that in the CTA module (average of  $2.8 \text{ Lm}^{-2}\text{h}^{-1}$ ), indicating that reverse flux assisted  
443 dissociation and dislodging of the foulant layer from the membrane surface could be more  
444 pronounced in the TFC FO membrane modules. The results in Fig. 7 (b) therefore have  
445 confirmed that the feed inlet pressure was dramatically decreased after osmotic backwashing  
446 and flushing the feed channel under the highest cross flow velocity for each module, i.e. from  
447 1.4 to 0.8 and from 0.35 to 0.25 for TFC and CTA modules, respectively. Still, the feed pressure  
448 was not restored to its original level for the clean module, thus indicating that almost full  
449 recovery was achieved or modification of the pressure balance in the module happened.

450 In order to compare the efficiency of the cleaning and estimate required durations for  
451 both modules, TOC concentrations flushed out of the module after each minute (i.e. 100 L) are  
452 presented in Fig. 7 (c). The results indicate that a very high load of foulants is removed in the  
453 early stage of physical cleaning and after 3 min (300 L), the TOC level returns to that of the  
454 incoming tap water and no more foulants are flushed out the module. As such, it is clear that  
455 for the foulants used in this study, only a very short period of physical cleaning is required after  
456 osmotic backwash. Consequently, the combination of osmotic backwash and physical cleaning  
457 has proven to be an efficient cleaning strategy for the SW FO modules.

458



**Fig. 7.** (a) Variation of reverse water flux and feed pressure drop with osmotic backwash operation time, (b) effect of osmotic backwash and physical cleaning on the feed inlet pressure recovery and (c) total organic carbon (TOC, mg/L) concentration as a function of the water volume flushed (L). Physical cleaning with maximum feed cross-flow velocity of 0.44 and 0.91 m/s for CTA and TFC, respectively was performed for 5 min using tap water. The TOC of the feed was around 94 mg/L.

#### 460 **4. Conclusions**

461 This study presented practical considerations of SW FO modules with different  
462 membrane properties (CTA and TFC). The evaluation of two modules was conducted to  
463 establish hydrodynamic conditions under different feed and draw flow rates. In addition, the  
464 performances of two SW FO modules under different operation modes (FO and PAO modes)  
465 were compared. Finally, the effectiveness of the combined osmotic backwash and physical  
466 cleaning on the flux recovery was evaluated. The following conclusions are drawn:

- 467 • The draw side of the CTA module was more sensitive to flow rate due to the use of permeate  
468 spacers thick tricot creating more resistance to the flux. The operation of the draw side of  
469 the TFC module is less restrictive thanks to a mesh spacer but then less mechanical support  
470 is provided to the feed stream in the module. Also, pressure transfer from the feed to the  
471 draw channel was observed in PAO operation due to the potential compaction and  
472 narrowing of the draw channel.
- 473 • Novel TFC membrane allow for higher permeation flux and is more responsive to hydraulic  
474 pressure (PAO)
- 475 • In FO and PAO modes, enhanced water permeation caused by the additional hydraulic  
476 pressure on the feed side of the TFC module led to less RSF which is beneficial for process  
477 efficiency and potentially to limit (RSF enhanced) fouling propensity.
- 478 • Fouling tests demonstrated that fouling occur even when only limited impact on permeation  
479 is observed. Pressure control can be an important indicator of fouling occurrence for  
480 practical SW FO operation.
- 481 • The combination of osmotic backwash and physical cleaning confirmed to be very efficient  
482 and easy to implement on a module scale. Nevertheless, it has to be acknowledged that  
483 further studies of effective cleaning strategies for FO process including chemical cleaning

484 have to be conducted for improvement of techno-economic assessment of FO by evaluating  
485 organic removal efficiency and feed inlet pressure recovery.

486

487 Although this study demonstrated that the application of PAO operation enables to enhance the  
488 water flux and to limit the RSF in both SW FO modules, further studies on the comprehensive  
489 assessment of the PAO process including long-term operations are required. This can help to  
490 define optimal design for FO and PAO processes to prevent the pressure and energy losses  
491 caused by fouling in the system.

492

### 493 **Acknowledgements**

494 The authors acknowledge the financial support of the National Centre of Excellence in  
495 Desalination Australia, which is funded by the Australian Government through the National  
496 Urban Water and Desalination Plan. This research was also supported by a grant (code 16IFIP-  
497 B088091-03) from Industrial Facilities & Infrastructure Research Program funded by Ministry  
498 of Land, Infrastructure and Transport of Korean Government. The research leading to these  
499 results has received funding from the People Programme (Marie Curie Actions) of the Seventh  
500 Framework Programme of the European Union (FP7/2007-2013) under REA grant agreement  
501 n° 600388 (TECNIOspring programme), and from the Agency for Business Competitiveness  
502 of the Government of Catalonia, ACCIO. Finally, the authors thank Hydration Technology  
503 Innovations and Toray chemical Korea Inc. for the 8040 FO membrane modules they provided.  
504

### 505 **References**

- 506 1. She, Q.; Wang, R.; Fane, A. G.; Tang, C. Y., Membrane Fouling in Osmotically Driven  
507 Membrane Processes: A Review. *Journal of Membrane Science* **2016**, *499*, 201-233.
- 508 2. Phuntsho, S.; Lotfi, F.; Hong, S.; Shaffer, D. L.; Elimelech, M.; Shon, H. K., Membrane scaling  
509 and flux decline during fertiliser-drawn forward osmosis desalination of brackish groundwater. *Water*  
510 *Research* **2014**, *57*, 172-182.
- 511 3. Lee, S.; Boo, C.; Elimelech, M.; Hong, S., Comparison of fouling behavior in forward osmosis  
512 (FO) and reverse osmosis (RO). *Journal of Membrane Science* **2010**, *365*, (1-2), 34-39.
- 513 4. Zhao, S.; Zou, L.; Tang, C. Y.; Mulcahy, D., Recent developments in forward osmosis:  
514 Opportunities and challenges. *Journal of Membrane Science* **2012**, *396*, 1-21.
- 515 5. Cath, T.; Childress, A.; Elimelech, M., Forward osmosis: Principles, applications, and recent  
516 developments. *Journal of Membrane Science* **2006**, *281*, (1-2), 70-87.
- 517 6. Phuntsho, S.; Shon, H. K.; Hong, S.; Lee, S.; Vigneswaran, S., A novel low energy fertilizer  
518 driven forward osmosis desalination for direct fertigation: Evaluating the performance of fertilizer draw  
519 solutions. *Journal of Membrane Science* **2011**, *375*, (1-2), 172-181.
- 520 7. McCutcheon, J. R.; McGinnis, R. L.; Elimelech, M., A novel ammonia-carbon dioxide forward  
521 (direct) osmosis desalination process. *Desalination* **2005**, *174*, (1), 1-11.

- 522 8. Phuntsho, S., A novel fertiliser drawn forward osmosis desalination for fertigation. *Doctoral*  
523 *dissertation* **2012**.
- 524 9. McCutcheon, J. R.; McGinnis, R. L.; Elimelech, M., Desalination by ammonia-carbon dioxide  
525 forward osmosis: Influence of draw and feed solution concentrations on process performance. *Journal*  
526 *of Membrane Science* **2006**, *278*, (1–2), 114-123.
- 527 10. Tan, C. H.; Ng, H. Y., A novel hybrid forward osmosis-nanofiltration (FO-NF) process for  
528 seawater desalination: Draw solution selection and system configuration. *Desalination & Water*  
529 *Treatment* **2010**, *13*, (1-3), 356-361.
- 530 11. Alturki, A.; McDonald, J.; Khan, S. J.; Hai, F. I.; Price, W. E.; Nghiem, L. D., Performance of  
531 a novel osmotic membrane bioreactor (OMBR) system: Flux stability and removal of trace organics.  
532 *Bioresource Technology* **2012**, *113*, 201-206.
- 533 12. Blandin, G.; Verliefde, A.; Comas, J.; Rodriguez-Roda, I.; Le-Clech, P., Efficiently Combining  
534 Water Reuse and Desalination through Forward Osmosis—Reverse Osmosis (FO-RO) Hybrids: A  
535 Critical Review. *Membranes* **2016**, *6*, (3), 37.
- 536 13. Kim, Y.; Chekli, L.; Shim, W.-G.; Phuntsho, S.; Li, S.; Ghaffour, N.; Leiknes, T.; Shon, H. K.,  
537 Selection of suitable fertilizer draw solute for a novel fertilizer-drawn forward osmosis–anaerobic  
538 membrane bioreactor hybrid system. *Bioresource Technology* **2016**, *210*, 26-34.
- 539 14. Wang, R.; Shi, L.; Tang, C. Y.; Chou, S.; Qiu, C.; Fane, A. G., Characterization of novel  
540 forward osmosis hollow fiber membranes. *Journal of Membrane Science* **2010**, *355*, (1–2), 158-167.
- 541 15. Wei, J.; Qiu, C.; Tang, C. Y.; Wang, R.; Fane, A. G., Synthesis and characterization of flat-  
542 sheet thin film composite forward osmosis membranes. *Journal of Membrane Science* **2011**, *372*, (1–  
543 2), 292-302.
- 544 16. Yip, N. Y.; Tiraferri, A.; Phillip, W. A.; Schiffman, J. D.; Elimelech, M., High Performance  
545 Thin-Film Composite Forward Osmosis Membrane. *Environmental Science & Technology* **2010**, *44*,  
546 (10), 3812-3818.
- 547 17. Gu, Y.; Wang, Y.-N.; Wei, J.; Tang, C. Y., Organic fouling of thin-film composite polyamide  
548 and cellulose triacetate forward osmosis membranes by oppositely charged macromolecules. *Water*  
549 *Research* **2013**, *47*, (5), 1867-1874.
- 550 18. Wang, Z.; Tang, J.; Zhu, C.; Dong, Y.; Wang, Q.; Wu, Z., Chemical cleaning protocols for thin  
551 film composite (TFC) polyamide forward osmosis membranes used for municipal wastewater  
552 treatment. *Journal of Membrane Science* **2015**, *475*, 184-192.
- 553 19. Geise, G. M.; Lee, H. S.; Miller, D. J.; Freeman, B. D.; McGrath, J. E.; Paul, D. R., Water  
554 purification by membranes: the role of polymer science. *Journal of Polymer Science Part B: Polymer*  
555 *Physics* **2010**, *48*, (15), 1685-1718.
- 556 20. Zhu, X.; Elimelech, M., Colloidal fouling of reverse osmosis membranes: measurements and  
557 fouling mechanisms. *Environmental Science & Technology* **1997**, *31*, (12), 3654-3662.
- 558 21. Vrijenhoek, E. M.; Hong, S.; Elimelech, M., Influence of membrane surface properties on  
559 initial rate of colloidal fouling of reverse osmosis and nanofiltration membranes. *Journal of Membrane*  
560 *Science* **2001**, *188*, (1), 115-128.
- 561 22. Luttmiah, K.; Verliefde, A. R. D.; Roest, K.; Rietveld, L. C.; Cornelissen, E. R., Forward  
562 osmosis for application in wastewater treatment: A review. *Water Research* **2014**, *58*, 179-197.
- 563 23. Kim, J. E.; Phuntsho, S.; Lotfi, F.; Shon, H. K., Investigation of pilot-scale 8040 FO membrane  
564 module under different operating conditions for brackish water desalination. *Desalination and Water*  
565 *Treatment* **2014**, *53*, (10), 2782-2791.
- 566 24. Kim, Y. C.; Park, S. J., Experimental study of a 4040 spiral-wound forward-osmosis membrane  
567 module. *Environmental Science & Technology* **2011**, *45*, (18), 7737-45.
- 568 25. McGinnis, R. L.; Hancock, N. T.; Nowosielski-Slepowron, M. S.; McGurgan, G. D., Pilot  
569 demonstration of the NH<sub>3</sub>/CO<sub>2</sub> forward osmosis desalination process on high salinity brines.  
570 *Desalination* **2012**, *312*, 67-74.
- 571 26. Schwinge, J.; Neal, P. R.; Wiley, D. E.; Fletcher, D. F.; Fane, A. G., Spiral wound modules and  
572 spacers: Review and analysis. *Journal of Membrane Science* **2004**, *242*, (1–2), 129-153.
- 573 27. Phuntsho, S.; Shon, H.; Hong, S.; Lee, S.; Vigneswaran, S.; Kandasamy, J., Fertiliser drawn  
574 forward osmosis desalination: the concept, performance and limitations for fertigation. *Reviews in*  
575 *Environmental Science and Bio/Technology* **2012**, *11*, (2), 147-168.

- 576 28. Hancock, N. T.; Xu, P.; Roby, M. J.; Gomez, J. D.; Cath, T. Y., Towards direct potable reuse  
577 with forward osmosis: Technical assessment of long-term process performance at the pilot scale.  
578 *Journal of Membrane Science* **2013**, *445*, 34-46.
- 579 29. Valladares Linares, R.; Li, Z.; Yangali-Quintanilla, V.; Li, Q.; Amy, G., Cleaning protocol for  
580 a FO membrane fouled in wastewater reuse. *Desalination and Water Treatment* **2013**, *51*, (25-27),  
581 4821-4824.
- 582 30. Valladares Linares, R.; Li, Z.; Abu-Ghdaib, M.; Wei, C.-H.; Amy, G.; Vrouwenvelder, J. S.,  
583 Water harvesting from municipal wastewater via osmotic gradient: An evaluation of process  
584 performance. *Journal of Membrane Science* **2013**, *447*, 50-56.
- 585 31. Arkhangelsky, E.; Wicaksana, F.; Chou, S.; Al-Rabiah, A. A.; Al-Zahrani, S. M.; Wang, R.,  
586 Effects of scaling and cleaning on the performance of forward osmosis hollow fiber membranes.  
587 *Journal of Membrane Science* **2012**, *415-416*, 101-108.
- 588 32. Blandin, G.; Verliefe, A. R.; Le-Clech, P., Pressure enhanced fouling and adapted anti-fouling  
589 strategy in pressure assisted osmosis (PAO). *Journal of Membrane Science* **2015**, *493*, 557-567.
- 590 33. Blandin, G.; Verliefe, A. R. D.; Tang, C. Y.; Childress, A. E.; Le-Clech, P., Validation of  
591 assisted forward osmosis (AFO) process: Impact of hydraulic pressure. *Journal of Membrane Science*  
592 **2013**, *447*, 1-11.
- 593 34. Sahebi, S.; Phuntsho, S.; Kim, J. E.; Hong, S.; Shon, H. K., Pressure assisted fertiliser drawn  
594 osmosis process to enhance final dilution of the fertiliser draw solution beyond osmotic equilibrium.  
595 *Journal of Membrane Science* **2015**, *481*, 63-72.
- 596 35. Luttmiah, K.; Harmsen, D. J. H.; Wols, B. A.; Rietveld, L. C.; Jianjun, Q.; Cornelissen, E. R.,  
597 Continuous and discontinuous pressure assisted osmosis (PAO). *Journal of Membrane Science* **2015**,  
598 *476*, 182-193.
- 599 36. Oh, Y.; Lee, S.; Elimelech, M.; Lee, S.; Hong, S., Effect of hydraulic pressure and membrane  
600 orientation on water flux and reverse solute flux in pressure assisted osmosis. *Journal of Membrane*  
601 *Science* **2014**, *465*, 159-166.
- 602 37. Duan, J.; Litwiller, E.; Pinnau, I., Solution-diffusion with defects model for pressure-assisted  
603 forward osmosis. *Journal of Membrane Science* **2014**, *470*, 323-333.
- 604 38. Kim, Y. C.; Kim, Y.; Oh, D.; Lee, K. H., Experimental Investigation of a Spiral-Wound  
605 Pressure-Retarded Osmosis Membrane Module for Osmotic Power Generation. *Environmental Science*  
606 *& Technology* **2013**, *47*, (6), 2966-2973.
- 607 39. Boo, C.; Elimelech, M.; Hong, S., Fouling control in a forward osmosis process integrating  
608 seawater desalination and wastewater reclamation. *Journal of Membrane Science* **2013**, *444*, 148-156.
- 609 40. Ang, W. S.; Lee, S.; Elimelech, M., Chemical and physical aspects of cleaning of organic-  
610 fouled reverse osmosis membranes. *Journal of Membrane Science* **2006**, *272*, (1), 198-210.
- 611 41. Phillip, W. A.; Yong, J. S.; Elimelech, M., Reverse Draw Solute Permeation in Forward  
612 Osmosis: Modeling and Experiments. *Environmental Science & Technology* **2010**, *44*, (13), 5170-5176.
- 613 42. Cipollina, A.; Micale, G., *Sustainable Energy from Salinity Gradients*. Woodhead Publishing:  
614 2016.
- 615 43. Shakaib, M.; Hasani, S.; Mahmood, M., Study on the effects of spacer geometry in membrane  
616 feed channels using three-dimensional computational flow modeling. *Journal of Membrane Science*  
617 **2007**, *297*, (1), 74-89.
- 618 44. Park, M.; Kim, J. H., Numerical analysis of spacer impacts on forward osmosis membrane  
619 process using concentration polarization index. *Journal of Membrane Science* **2013**, *427*, 10-20.
- 620 45. Kim, Y. C.; Elimelech, M., Adverse impact of feed channel spacers on the performance of  
621 pressure retarded osmosis. *Environmental Science & Technology* **2012**, *46*, (8), 4673-4681.
- 622 46. Coday, B. D.; Heil, D. M.; Xu, P.; Cath, T. Y., Effects of transmembrane hydraulic pressure on  
623 performance of forward osmosis membranes. *Environmental Science & Technology* **2013**, *47*, (5),  
624 2386-2393.
- 625 47. Blandin, G.; Verliefe, A. R.; Tang, C. Y.; Le-Clech, P., Opportunities to reach economic  
626 sustainability in forward osmosis–reverse osmosis hybrids for seawater desalination. *Desalination*  
627 **2015**, *363*, 26-36.

- 628 48. Xie, M.; Nghiem, L. D.; Price, W. E.; Elimelech, M., Impact of humic acid fouling on  
629 membrane performance and transport of pharmaceutically active compounds in forward osmosis. *Water*  
630 *Research* **2013**, *47*, (13), 4567-4575.
- 631 49. Mi, B.; Elimelech, M., Chemical and physical aspects of organic fouling of forward osmosis  
632 membranes. *Journal of Membrane Science* **2008**, *320*, (1-2), 292-302.
- 633 50. Achilli, A.; Cath, T. Y.; Childress, A. E., Selection of inorganic-based draw solutions for  
634 forward osmosis applications. *Journal of Membrane Science* **2010**, *364*, (1), 233-241.
- 635 51. Phuntsho, S.; Kim, J. E.; Johir, M. A. H.; Hong, S.; Li, Z.; Ghaffour, N.; Leiknes, T.; Shon, H.  
636 K., Fertiliser drawn forward osmosis process: Pilot-scale desalination of mine impaired water for  
637 fertigation. *Journal of Membrane Science* **2016**, *508*, 22-31.
- 638 52. Blandin, G.; Vervoort, H.; Le-Clech, P.; Verliefde, A. R. D., Fouling and cleaning of high  
639 permeability forward osmosis membranes. *Journal of Water Process Engineering* **2016**, *9*, 161-169.
- 640 53. Mi, B.; Elimelech, M., Organic fouling of forward osmosis membranes: Fouling reversibility  
641 and cleaning without chemical reagents. *Journal of Membrane Science* **2010**, *348*, (1), 337-345.
- 642 54. Tang, C. Y.; Fu, Q. S.; Criddle, C. S.; Leckie, J. O., Effect of flux (transmembrane pressure)  
643 and membrane properties on fouling and rejection of reverse osmosis and nanofiltration membranes  
644 treating perfluorooctane sulfonate containing wastewater. *Environmental Science & Technology* **2007**,  
645 *41*, (6), 2008-2014.